Heliyon 10 (2024) e33152

Contents lists available at ScienceDirect

Heliyon

journal homepage: www.cell.com/heliyon

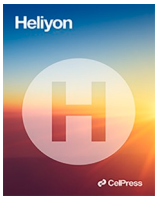

Research article

The impact of gut microbial dysbiosis on the atrophy of the hippocampus and abnormal metabolism of N-acetyl aspartate in type 2 diabetic rats

Zhenyang Zhu [a,1], Qingqing Chen [b,1], Gege Jiang [c], Yuan Liang [d], Jing Shen [c,*], Jianlin Wu [c,**]

[a] Department of Radiology, Panzhihua Central Hospital, Panzhihua, China
[b] Department of Radiology, Yiwu Central Hospital, Yiwu, China
[c] Department of Radiology, Affiliated Zhongshan Hospital of Dalian University, Dalian, China
[d] Department of Radiology, The Second Affiliated Hospital of Chongqing Medical University, Chongqin, China

ARTICLE INFO

Keywords:
Rat model
Streptozotocin
Microbiota
Intestinal
MRI
^{1}H-MRS
Type 2 diabetes mellitus

ABSTRACT

Rationale and objectives: This study aimed to investigate the effect of intestinal dysbiosis on the hippocampal volume using proton magnetic resonance spectroscopy (^{1}H-MRS) in a type 2 diabetes mellitus (T2DM) rat model.

Materials and methods: We established a T2DM animal model with high-fat diet and streptozotocin (HFD/STZ) administration to Sprague-Dawley rats. Short-term ceftriaxone sodium administration was used to establish a T2DM intestinal dysbiosis (T2DM-ID) model. After establishing the model, fecal microbiota were detected using 16S rRNA sequencing. The models were then subjected to magnetic resonance imaging (MRI). Associations between MRI findings and fecal microbiota were evaluated.

Results: Magnetic resonance imaging (MRI) showed that the bilateral hippocampal voxel value and N-acetylaspartate (NAA) level were lower in the experimental group than in the normal control (NC) group ($p < 0.05$) and that NAA/creatine in the left hippocampus was lower in the T2DM-ID group than in the NC group ($p < 0.05$). α and β diversities differed significantly among the three groups ($p < 0.05$). In the T2DM and T2DM-ID groups, the abundance of bacteria in the phylum *Proteobacteria* increased significantly, whereas that of bacteria in the phylum *Firmicutes* decreased. The relative abundance of *Actinobacteria* was significantly increased in the T2DM-ID group. The Chao1 index ($r = 0.33$, $p < 0.05$) and relative abundance of *Firmicutes* ($r = 0.48$, $p < 0.05$) were positively correlated with the left hippocampal voxel, while the relative abundance of *Proteobacteria* was negatively correlated with the left hippocampal voxel ($r = -0.44$, $p < 0.05$). NAA levels, bilateral hippocampal voxels, and the relative abundance of *Lactobacillus*, *Clostridia_UCG_014*, and other genera were correlated positively ($r = 0.34$–0.70, $p < 0.05$). NAA levels and the relative abundances of *Blautia* and *Enterococcus* were correlated negatively ($r = -0.32$–0.44, $p < 0.05$).

* Corresponding author.
** Corresponding author.
E-mail addresses: Dsqshenjing2002@163.com (J. Shen), cjr.wujianlin@vip.163.com (J. Wu).
[1] These authors share first authorship.

https://doi.org/10.1016/j.heliyon.2024.e33152
Received 17 June 2022; Received in revised form 12 June 2024; Accepted 14 June 2024
Available online 15 June 2024

Conclusion: The T2DM-ID rat model showed hippocampal volume atrophy and decreased levels of neuronal markers (such as NAA). The abnormal content of specific gut microorganisms may be a key biomarker of T2DM-associated brain damage.

Abbreviations

Cho	choline (Cho)
Cr	creatine
NC	normal control
T2DM	type 2 diabetes mellitus
T2DM-ID	type 2 diabetes mellitus intestinal dysbiosis
GBA	gut–brain axis
OTUs	operational taxonomic units
HV	hippocampal voxel
NAA	N-acetylaspartate
STZ	streptozotocin

1. Introduction

Diabetes mellitus (DM) is a systemic metabolic disease characterized by hyperglycemia that affects a large proportion of the population, particularly younger individuals [1]. According to the 10th edition of the World Diabetes Map, the global prevalence of DM will be 537 million in 2021, accounting for 10 % of the world's total population, and is projected to increase continually [2]. DM, particularly type 2 DM (T2DM), imposes economic burdens on patients and their families and has detrimental effects on society. Long-term T2DM is associated with multisystem systemic complications, making its treatment and management complex and challenging. Based on the gut–brain axis (GBA) two-way communication theory, intestinal microbes in T2DM may affect the central nervous system through the neuroendocrine and neuroimmune pathways. This interaction is associated with increased risks of dementia, cerebrovascular disease, and brain atrophy in patients with T2DM. However, the specific pathological mechanism remains unclear [3–5].

This study sought to establish a T2DM animal model through HFD/STZ, with intestinal microbiota change via ceftriaxone sodium administration [6–10]. We hypothesized that dysbiosis in T2DM affects brain structure and function and evaluated the intestinal microbiota of T2DM model rats with the 16S rRNA sequencing technique. Brain structural magnetic resonance imaging (sMRI) and proton magnetic resonance spectroscopy (^{1}H-MRS) were performed. Combining intestinal microecology and medical imaging to study the effects of T2DM gut microbiota on brain structure and function may improve our understanding of the etiology of T2DM and provide a theoretical basis for the search and development of targeted biological agents.

2. Materials and methods

2.1. Animals

Forty-five male Sprague–Dawley (SD) rats weighing 200 ± 20 g (age, 8 weeks) were used. Specific pathogen-free rats were purchased from Liaoning Changsheng Biotechnology Co., Ltd. (Animal License No: SCXK [Liaoning] 2020-0001). All experimental animals were raised in a barrier environment. The animals were housed in standard polypropylene cages (five rats/cage) and maintained under controlled room temperature and humidity with a 12/12-h light-dark cycle. Animals were randomly divided into three groups: normal control (NC, $n = 10$), T2DM, and T2DM intestinal dysbiosis (T2DM-ID) groups. For adaptation, all rats were enrolled in a familiarization period of 1 week. During this period, they were provided with a common rat diet, and Fasting blood glucose (FBG) was checked at the start and end of the familiarization period to evaluate the health status. After the familiarization period, all NC groups were fed with a normal pellet diet (NPD), while the T2DM and T2DM-ID groups were fed with a high-fat diet (HFD) until the end of the experiment. Animal food was purchased from Xiaoshuyoutai (Beijing) Biotechnology Co., Ltd. (License No.: SCXK [Beijing] 2018-0006). The animal experiments were approved by the Ethics and Welfare Ethics Review Committee of the Animal Experiment Center, Zhongshan Hospital Affiliated with Dalian University (Approval No.: 202104012). The study protocol and report complied with all regulations.

2.2. Intervention

A T2DM rat model was established by 5 weeks of high-fat diet combined with a single intraperitoneal injection of 40 mg/kg STZ (Coolaber, Beijing, China). STZ was dissolved in a 0.1 mol/L sodium citrate buffer (pH 4.2–4.5) and injected within 30 min. FBG were

measured using rat tail vein blood sampling. FBG levels and body weight were measured weekly. Each rat was fasted overnight, and FBG was measured from tail blood using a glucometer (Roche Diagnostics GmbH, Germany) and glucose strips (Accu Chek Performa, United States). The body weight was measured using a weight balance and expressed in grams [11,12]. FBG ≥8.3 mmol/L 72 h after administration suggested that a T2DM rat model had been established (6). The T2DM-ID models were established by gavage of ceftriaxone sodium (North China Pharmaceutical, Hebei, China) at a continuous low dose (1 mg/mL, once/day) for 1 week in T2DM rat models [7,10–13]. In contrast, each rat in the NC and T2DM groups was administered with 1 mL of distilled water. Rats that did not meet the inclusion criteria were excluded.

2.3. Microbiota methods and measures

Rat fecal samples were collected by massaging the perineum after establishing the models. Fecal pellets were collected weekly between 9:00 a.m. and 9:30 a.m., snap-frozen, and stored at −80 °C. Only fresh fecal samples discharged from the anus of the massaged rats were collected and transferred to a clean 5-mL cryopreservation tube. Genomic DNA of 50-mg samples was extracted using cetyltrimethylammonium bromide. Subsequently, the V3 + V4 variable region of the 16S rRNA gene was amplified using primers 341 F (5′-CCTAYGGGRGCAS-3′) and 806R (5′-GGACTACNNGGGTATCTAAT-3′). PCR products were purified using the QIAEX II Gel Extraction Kit (Qiagen, Hilden, Germany). Finally, a DNA library was constructed using the Illumina TruSeq® DNA PCR-Free Sample Preparation Kit (Illumina, California, USA). The constructed library was then subjected to Qubit quantification and library detection. After quantification, NovaSeq 6000 PE250 was used for on-machine sequencing [14]. Original sequences were processed according to the Qiime2 tutorial [15]. The DADA2 plugin was used for quality control, trimming, denoising, splicing, and chimera removal, and the final feature sequence list was obtained [16]. Subsequently, the feature-classifier plug-in was used to align the representative sequences of ASV to the 99 % similarity SILVA database (according to the 341F/806R primer pair used to trim the database to the V3V4 region) and to obtain taxonomic information of the species [17]. Finally, all contaminating mitochondrial and chloroplast sequences were removed using the QIIME2 feature table plugin. The Chao1 and Shannon indices, which represent the richness and diversity of the sample, respectively, were chosen as α diversity indices at the feature sequence level. β diversity was calculated using the Bray-Curti index to evaluate differences in the microbial community structure between samples, which were then displayed using a principal coordinate analysis (PCoA) map [18]. The linear discriminant analysis effect size (LEfSe) was used to evaluate differences in bacterial taxa between the two experimental groups. Bacterial phyla and genera with significant differences were selected for a correlation analysis to link intestinal flora with brain MRI parameters.

2.4. MRI examination

MRI data were collected using Verio 3.0T superconducting magnetic resonance (Siemens Healthineers, Munich, Germany) with an eight-channel coil array specific to rats (ChenGuang Medical Science and Technology, Shanghai, China). The two experimental groups underwent MRI 7–8 weeks after STZ administration. Before MRI, the animals were anesthetized with an intraperitoneal injection of chloral hydrate as a 10 % aqueous solution (0.3 mL/100 g). The rats were placed in the prone position with their heads at the center of the coil. The axial scanning range included the entire head area. The main scanning parameters were: (1) T1WI: TR = 1900 ms, TE = 3.56 ms, slice thickness = 0.40 mm, slice spacing = 0.40 mm, FOV = 80 × 80 mm, and scan matrix = 256 × 256; (2) Multivoxel ^{1}H-MRS scan: TR = 1700 ms, TE = 135 ms, flip angle = 90°, layer thickness = 5 mm, and FOV = 55 × 55 mm. After MRI data acquisition, the original image was spatially corrected using MATLAB 2016 (MathWorks, Massachusetts, USA) and enlarged to × 20 voxels. Subsequently, the ITK-SNAP auxiliary annotation tool was used to delineate the bilateral hippocampi in the layers on the T1WI map, and the hippocampal voxels (HVs) were calculated using the software plug-in. The ^{1}H-MRS scan quantitatively detected metabolic markers in the bilateral hippocampi to evaluate functional changes in rat hippocampi. Metabolic markers included N-acetylaspartate (NAA), choline (Cho), and creatine (Cr). The NAA/Cr and NAA/Cho ratios were calculated using 3.0T magnetic resonance post-processing workstation.

2.5. Statistical analysis

Data were analyzed using the IBM Statistical Package for the Social Sciences version 20 (SPSS Inc., Chicago, IL, USA). Unpaired *t*-test, Mann–Whitney *U* test, one-way ANOVA, and Kruskal–Wallis test were used for statistical analyses. Metrology data are expressed as mean ± standard deviation. Datasets such as HV and NAA were analyzed using one-way ANOVA or Kruskal–Wallis tests with Bonferroni post-hoc tests, when appropriate. α diversity indices (Chao1 and Shannon) were analyzed to investigate dissimilarity in each group. The PCoA plot based on QIIME 2 software assessed variations in the species composition between groups. β diversity was analyzed using Permanova-S with 999 permutations [19]. LEfSe was calculated using the micro-in-cloud online analysis program based on the Galaxy module (https://www.bioincloud.tech/) [20], and the linear discriminant analysis (LDA) discriminative feature score threshold was set to 4.0. Pearson's correlation coefficients between the microbial composition and key MRI findings were calculated ($p < 0.05$, considered statistically significant) and plotted using Origin 2021. The statistical outliers were excluded from the dataset.

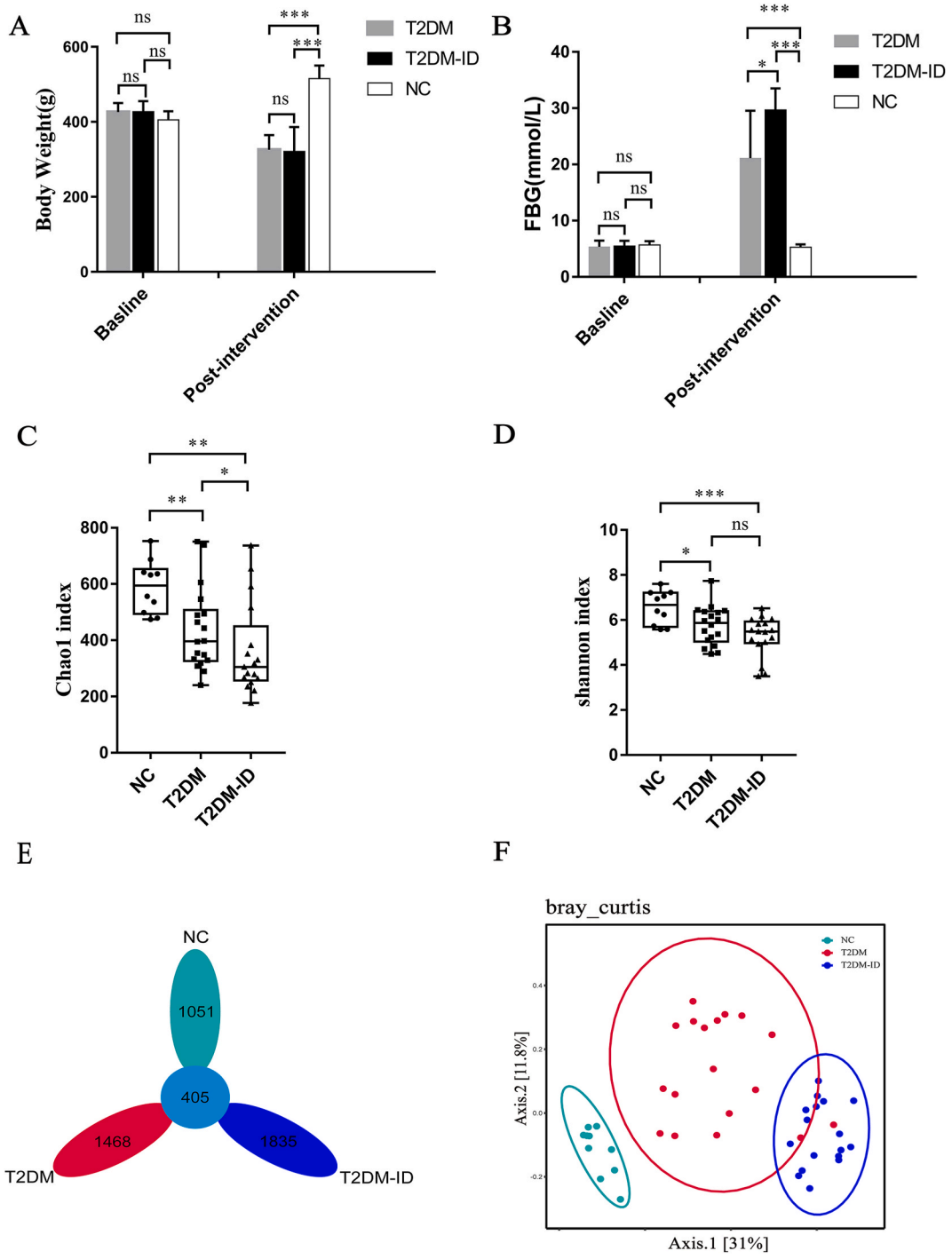

Fig. 1. Comparison of body weight and FBG at baseline and Post-intervention (A and B). Microbial analyses. (C and D) Comparison of diversity in microbiota fecal samples among NC, T2DM, and T2DM-ID rats using alpha diversity measures (Chao1 index and Shannon Index). (E) The Venn diagram shows the OTU unique to each sample and the OUT shared by different samples. (F) The principal coordinate analysis plot of Bray-Curti distances showing a clear separation in microbial composition among NC, T2DM, and T2DM-ID groups. *$p < 0.05$; **$p < 0.01$; ***$p < 0.001$.

3. Results

3.1. Changes in body weight and FBG levels among the three groups

Before modeling, baseline body weight differed significantly among NC (405.2 ± 23.2 g), T2DM (426.1 ± 24.1 g), and T2DM-ID (427.4 ± 27.8 g) groups ($p = 0.066$). After the establishment of the model, the body weights of T2DM (316.9 ± 41.7 g) and T2DM-ID (321.2 ± 65.0 g) rats in the model group were significantly lower than those of NC rats (515.4 ± 35.0 g; $p < 0.001$), but the body weight did not differ significantly between T2DM and T2DM-ID rats ($p = 0.836$) (Fig. 1A). Similar to body weight, baseline FBG levels did not differ significantly among NC (5.7 ± 0.7 mmol/L), T2DM (5.2 ± 1.1 mmol/L), and T2DM-ID (5.7 ± 0.9 mmol/L) groups before modeling ($p = 0.627$). After the establishment of the model, the FBG levels of T2DM (21.3 ± 8.4 mmol/L) and T2DM-ID (29.7 ± 3.8 mmol/L) rats were significantly higher in the model group than in the NC group (5.3 ± 0.5 mmol/L; $p < 0.001$), and the FBG levels of T2DM-ID rats were also significantly higher than those of T2DM rats ($p = 0.018$) (Fig. 1B). In addition, rats in the model group showed obvious polydipsia, polyuria, and sparse hair.

3.2. Changes in fecal bacteria in T2DM-ID rat models

Operational taxonomic unit (OUT) assessment of alpha and beta diversity indices showed marked variation between the groups. Within-sample diversity (α-diversity) showed significant differences among NC, T2DM, and T2DM-ID rats ($p < 0.05$). Between-group differences were significant between NC and T2DM (Chao1 index: $H = 8.002$, $p = 0.005$; Shannon index: $H = 4.655$, $p = 0.031$), NC and T2M-ID (Chao1 index: $H = 9.076$, $p = 0.003$; Shannon index: $H = 10.651$, $p = 0.001$), and T2DM and T2MD-ID (Chao1 index: $H = 4.187$, $p = 0.041$; Shannon index: $H = 1.573$, $p = 0.210$) (Fig. 1C and D). The Venn plot showed 1051 unique OTUs in the NC group, 1468 unique OTUs in the T2DM group, and 1835 unique OTUs in the T2DM-IDs group. A total of 405 OTUs were shared among the three groups (Fig. 1E). β-diversity differed significantly among the NC, T2DM, and T2DM-ID groups (PERMANOVA, $p < 0.001$). The NC group was clustered separately from the T2DM and T2DM-ID groups in the PCoA plot (Fig. 1F).

At the phylum level, the intestinal microbiota compositions of the three groups differed, with *Firmicutes* being the most abundant phylum (Fig. 2A). Between the groups, the relative abundances of phyla (4) and genera (16) showed numerous variations. The

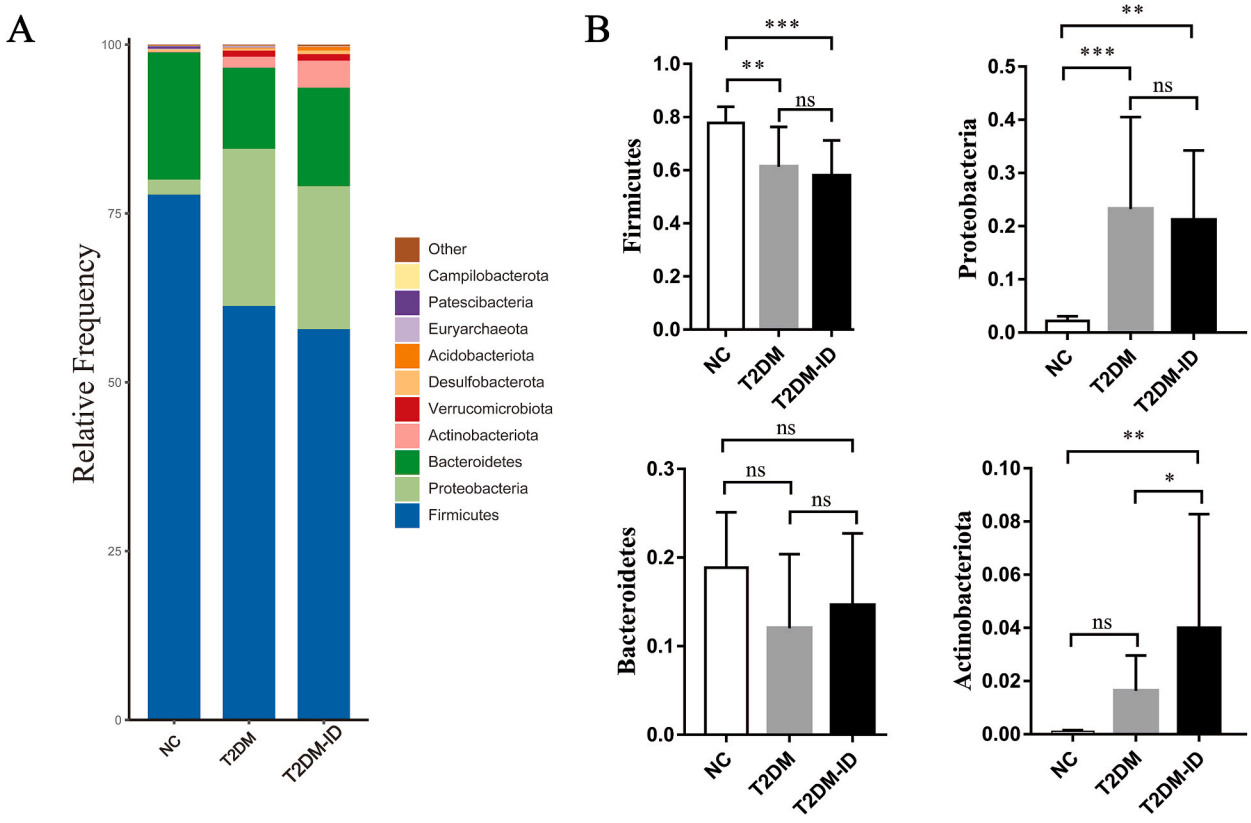

Fig. 2. Differences in phylum-level bacterial community compositions among the three groups. (A) Distribution of the top 10 species with the highest abundance levels in each group. (B) The top four dominant phylums with the highest abundance were compared among groups. *$p < 0.05$; **$p < 0.01$; ***$p < 0.001$.

abundance of *Firmicutes* was significantly higher in the NC group than in the T2DM and T2DM-ID groups ($F = 17.81$, $p < 0.001$). The abundances of *Proteobacteria* ($F = 29.98$, $p < 0.001$) and *Actinobacteria* ($F = 18.26$, $p < 0.001$) were significantly lower in the NC group than those in the T2DM and T2DM-ID groups. The relative abundance of *Actinobacteria* was significantly lower in the T2DM group than in the T2DM-ID group. The *Bacteroidetes* abundance did not differ significantly among the three groups ($F = 2.43$, $p = 0.100$; Fig. 2B). The Firmicutes/Bacteroidetes ratio did not demonstrated significant difference among the three groups (NC: 4.8 ± 2.5, T2DM: 9.4 ± 8.7, T2DM-ID: 6.3 ± 6.3, $F = 2.20$, $p = 0.130$).

At the genus level, *Lactobacillus, Romboutsia*, *Turicibacter*, *Muribaculaceae*, *Clostridium_sensu_stricto_1*, *Clostridia_UCG_014*, *Lachnospiraceae_NK4A136_group*, and *Rumincoccus* decreased significantly in the T2DM and T2DM-ID groups compared to the NC group. Moreover, *Blautia* and *Escherichia_Shigella* species significantly declined in NC and T2DM-ID groups. In contrast, *Megamonas*, *Klebsiella*, *Phascolarctobacterium*, *Prevotella*, *Bifidobacterium*, and *Enterococcus* significantly increased in the T2DM-ID group. The LEfSe analysis cladogram showed that the aforementioned 16 genera differed in relative abundance among the three groups (LAD score >4.0, $p <$ 0.05; Fig. 3A and B).

3.3. Changes in hippocampal morphology and NAA in the T2DM-ID rat model

The bilateral HVs differed among the NC, T2DM, and T2DM-ID groups ($p < 0.05$). The T2DM group (left: 604 ± 59; right: 593 ± 79) had lower bilateral HVs compared to the NC group (left: 801 ± 102; right: 800 ± 49; $p = 0.000$). The T2DM-ID group (left: 623 ± 142; right: 598 ± 126) had lower bilateral HVs than the NC group ($p = 0.000$). However, the bilateral HVs did not differ significantly between the T2DM and T2DM-ID groups ($p > 0.05$; Fig. 4A and B).

The bilateral hippocampal NAA differed among the three groups ($p < 0.05$). The T2DM (left: 0.085 ± 0.028; right: 0.070 ± 0.025) and T2DM-ID groups (left: 0.085 ± 0.028; right: 0.077 ± 0.031) had lower NAA than the NC group (left: 0.121 ± 0.023; right: 0.115 ± 0.026; $p < 0.05$). NAA levels did not differ significantly between the T2DM and T2DM-ID groups ($p > 0.05$), whereas the NAA/Cr ratio in the left hippocampus of the T2DM-ID group (0.978 ± 0.240) was lower than that in the NC group (1.394 ± 0.368; $p = 0.015$). The other ^{1}H-MRS parameters, Cho, Cr, and NAA/Cr, did not differ among the three groups ($p > 0.05$; Fig. 4C–E).

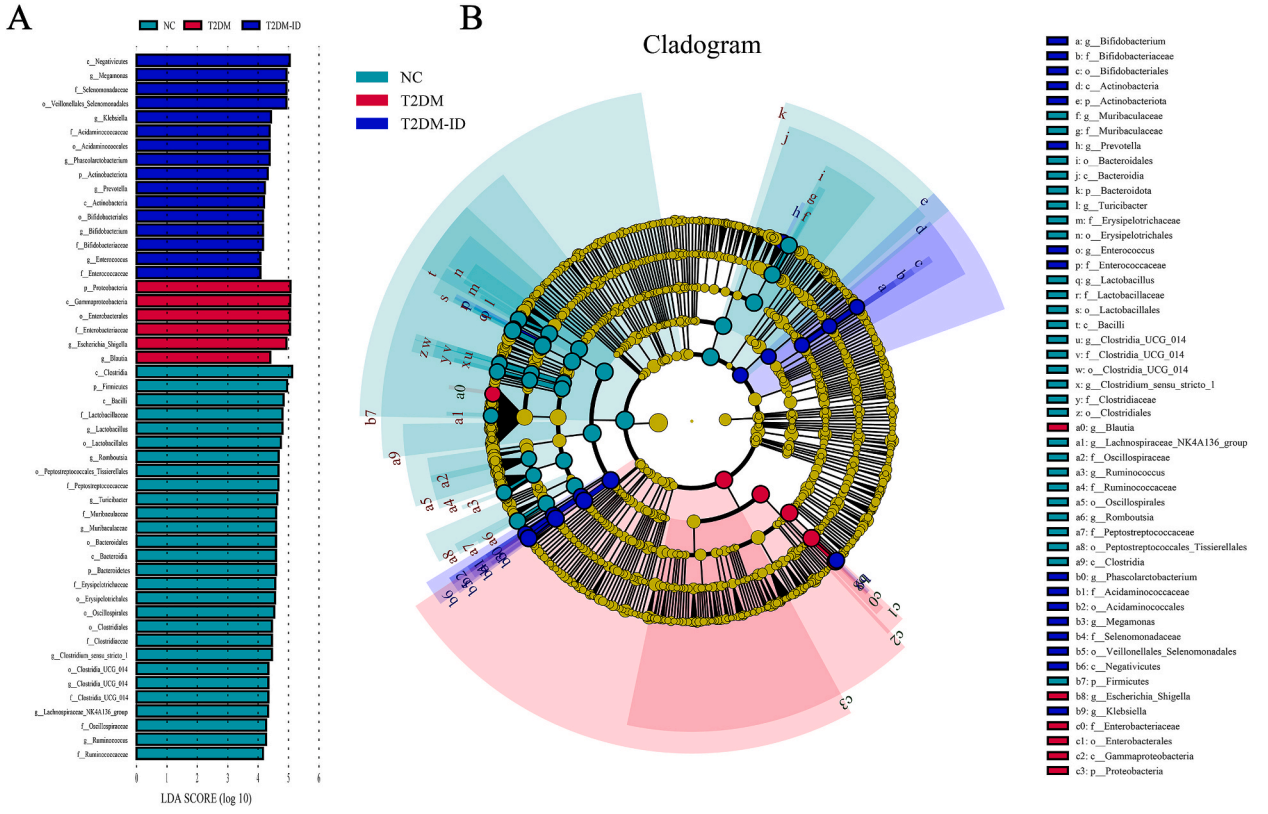

Fig. 3. Group biomarkers. (A) LDA score (LDA >4.0, $p < 0.05$) for the LEfSe analysis shows the significantly enriched species and their importance in each group. (B) Cladogram plots analyzed by LEfSe show the evolutionary laws of the branches of species that play an important role in each set of samples.

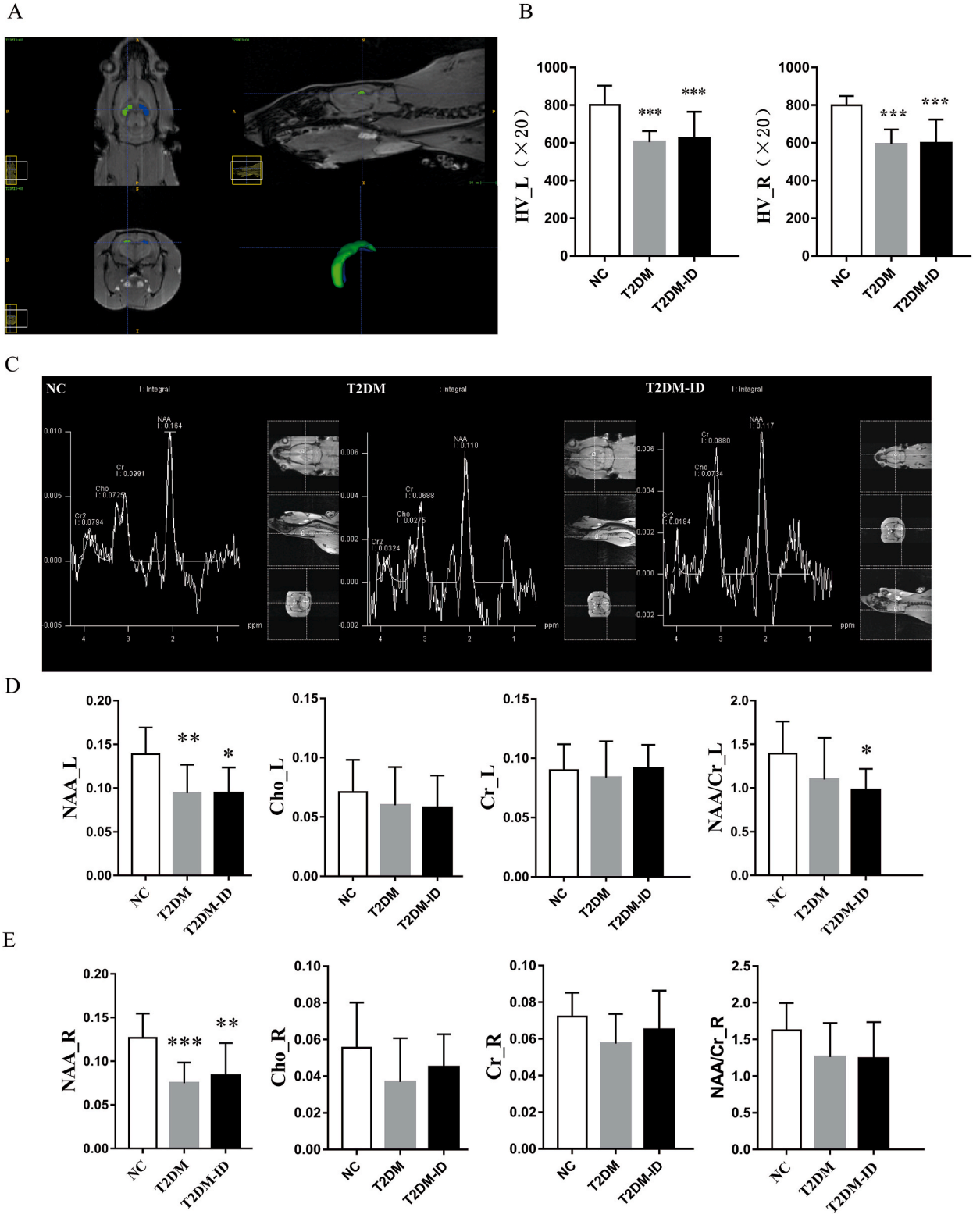

(caption on next page)

Fig. 4. Magnetic resonance image processing example and results. (A) Schematic diagram of labeling rat hippocampus with ITK-SNAP software. (B) Bilateral HVs of T2DM and T2DM-ID rats were significantly lower than those of NC rats. (C) Example diagrams of 1H-MRS in the hippocampi of NC, T2DM, and T2DM-ID rats. (D, E) Bilateral hippocampal NAA levels of T2DM and T2DM-ID rats were significantly lower than those of the NC group. The NAA/Cr in the left hippocampus of T2DM-ID rats was significantly lower than that of NC rats. Cho, Choline; Cr, Creatine; HV, hippocampal voxels; L, left; NAA, N-acetylaspartate; R, right. *$p < 0.0$; **$p < 0.01$; ***$p < 0.001$.

3.4. Microbiota changes associated with abnormal hippocampal morphology and NAA

The Chao1 index was positively correlated with the left HV ($r = 0.33$, $p = 0.038$). The relative abundance of *Firmicutes* was positively correlated with the left HV ($r = 0.48$, $p = 0.002$). *Proteobacteria* were negatively correlated with the left HV (r = −0.44, p = 0.005). At the genus level, *Blautia* was negatively correlated with bilateral HV, NAA, and NAA/Cr ($r = -0.36$ to -0.44, $p < 0.05$); *Enterococcus* was negatively correlated with bilateral HV (L: $r = -0.32$, R: $r = -0.36$, $p < 0.05$); and *Megamonas* was negatively correlated with right HV ($r = -0.36$, $p = 0.025$). *Escherichia Shigella* was negatively correlated with the left HV ($r = -0.46$, $p = 0.003$). Genera including *Lactobacillus*, *Clostridia UCG 014*, *Clostridium_sensu_stricto_1*, *Muribaculaceae*, *Lachnospiraceae_NK4A136_group*, *Turicibacter*, *Ruminococcus*, and *Romboutsia* were positively correlated with bilateral HV, NAA, and NAA/Cr (L: $r = 0.34$–0.70, $p < 0.05$; Fig. 5).

4. Discussion

Based on the theory of GBA bidirectional communication, a link has been demonstrated between gut microbes and a range of metabolic and neuropsychiatric disorders [21–24]. Herein, we hypothesized that intestinal dysbiosis in a T2DM rat model affects brain structure and function. The results showed that the hippocampi of the T2DM-ID rat model atrophied to varying degrees and that the content of the hippocampal ^{1}H-MRS neural marker NAA decreased to varying degrees.

HFD/STZ is a reliable method for establishing an animal model of T2DM. Despite the long modeling period, the model was more similar to the pathological state of human T2DM [25–27]. In this study, the body weight of rats in the model group was significantly lower than that of NC rats ($p < 0.05$), but the FBG level was significantly higher than that of NC rats ($p < 0.05$) and accompanied by

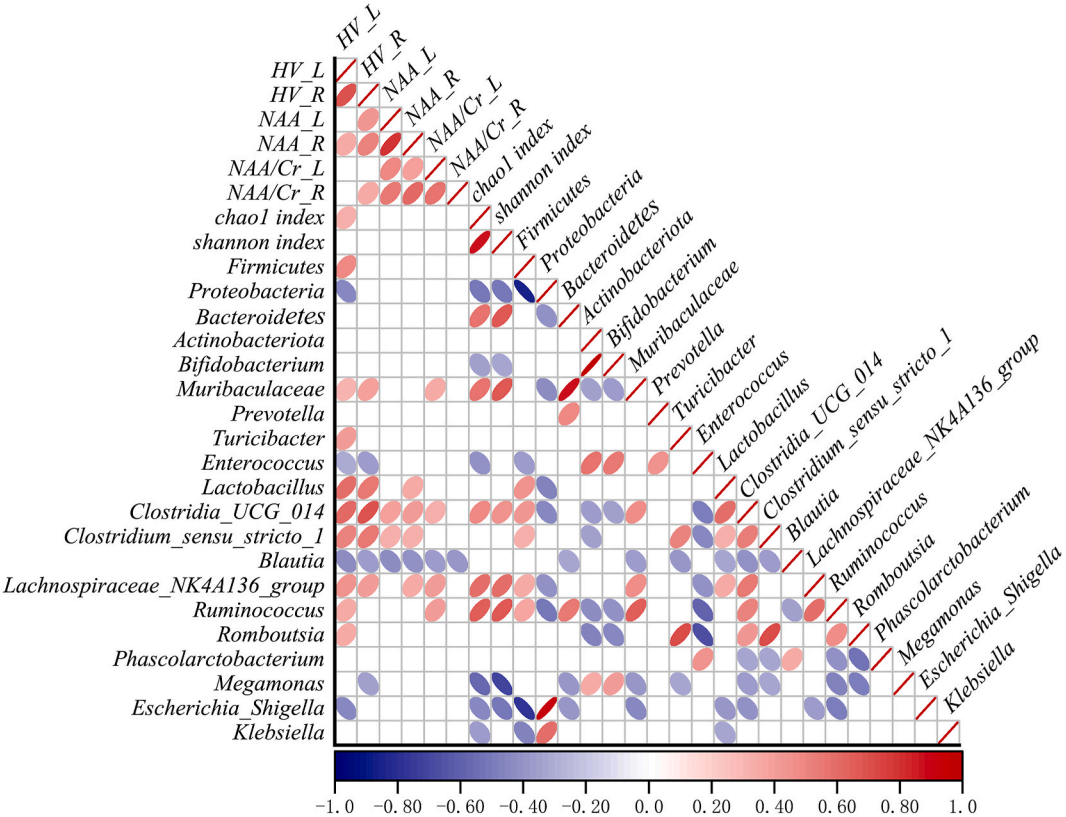

Fig. 5. Correlations between key neurobiological findings and bacterial genera. Pearson correlations between relative taxa abundance and rat bilateral HV, NAA, and NAA/Cr indices. All correlations presented were statistically significant ($p < 0.05$) with strong correlations indicated by lines and weaker correlations by circles. Colors denote whether correlations are negative (blue) or positive (red).

diabetes symptoms, indicating that the model was successfully established [7,8,10–12]. The FBG level of T2DM-ID rats was also significantly higher than that of T2DM rats ($p < 0.05$), indicating that further imbalance of intestinal flora based on T2DM makes FBG more difficult to control, and some bacteria may play an important role. Several recent studies [26–28] based on intestinal flora and blood glucose control in patients with T2DM have confirmed that abnormalities in certain bacterial abundances, such as increased *Enterococcus* abundance, affect FBG levels. When analyzing the fecal samples of each group of rats, we were surprised to find that the number of OTUs in the fecal samples of the T2DM and T2DM-ID groups was higher than that of NC rats, which differed from the results of Almugadam et al. [11] However, similar to previous studies [24,28], we found that the α-diversity index of the T2DM rat model was lower than that of normal rats ($p < 0.05$). The α-diversity index of T2DM-ID rats after intragastric administration of ceftriaxone sodium was the lowest among the three groups; it was significantly lower than that of the NC group ($p < 0.05$) but did not differ from that of the T2DM group ($p > 0.05$). However, the flora richness index (Chao1 index) of the T2DM-ID group was lower than that of the other groups ($p < 0.05$). Further comparison of β-diversity revealed that the relative abundance of bacteria from seven phyla and 16 genera differed among the three groups ($p < 0.05$). Consistent with previous studies [29–31], the relative abundance of bacteria in the phylum *Proteobacteria* in the T2DM group was significantly increased, but the relative abundance of bacteria in the phylum *Firmicutes* was significantly decreased. Others [32,33] have found that lipopolysaccharides in the cell wall of *Proteobacteria* are involved in autoimmunity and that their relative abundance may be related to the enhanced immune mechanism of the GBA in T2DM-related brain injury. In addition, the relative abundance of *Actinobacteria* significantly increased in the T2DM-ID group in this study, confirming that short-term low-dose ceftriaxone sodium gavage can change the structure of the intestinal flora in the T2DM rat model, resulting in a T2DM-ID model [7]. The Firmicutes/Bacteroidetes ratio is frequently cited as a hallmark of T2DM and other metabolic diseases in the scientific literature [34,35]. Moreover, it has been proposed that the ratio of Firmicutes/Bacteroides in the intestine increases when the body is in a pathological state, because the Firmicutes phylum has better resistance to harsh environments [27,29,35,36]. In the present research, the ratio of Firmicutes/Bacteroides in the experimental group was higher than that in the NC group, however, there was no significant difference. We believe that more satisfactory results can be obtained if the experimental time is further extended and the sample size is increased. The aforementioned results show that the accumulation of biological quantity is not always beneficial, and increase in species richness and diversity is important for maintaining the balance of the ecosystem, which is also applicable to intestinal microecosystems [37–39]. Some dominant microorganisms in T2DM rats, such as *Proteobacteria* and *Actinobacteria*, may be key microbial markers for T2DM-related complications.

The hippocampus is a key brain region involved in neural activities, including cognition, memory, and emotion regulation. It is sensitive to age, stress, metabolic abnormalities, and even changes in the composition of gut microbes [40–42]. In this study, the hippocampus was selected as the main brain region of interest to investigate differences in brain structure and function among the NC, T2DM, and T2DM-ID groups. Similar to previous studies [43–45], it was revealed that compared to NC rats, the bilateral hippocampal volumes of T2DM and T2DM-ID rats were atrophied to varying degrees. Model rat activity slowed following STZ administration, but the sniffing action increased, which may be related to hippocampal damage. HV did not differ significantly between the T2DM and T2DM-ID groups ($p > 0.05$). Although pathological abnormalities may be present in the hippocampi of the T2DM-ID model rats, no morphological abnormalities were identified. T2DM is a persistent metabolic disease, without complete cure at present. Once diagnosed, it may persist throughout the lifetime in patients with T2DM [46,47]. In this study, the experimental group was only observed 7–8 weeks after modeling, and the damage caused by flora imbalance to the central nervous system in T2DM and T2DM-ID rats may not be more manifested. In the future, the use of MRI equipment with higher field strength will enable the detection of related abnormalities of the central nervous system in the early stages of T2DM [48–50].

To explore the differences in hippocampal function and metabolism in the T2DM-ID rat models, the relevant metabolites in the bilateral hippocampi of rats were investigated using ^{1}H-MRS, which is the only functional sequencing method that can clearly evaluate metabolite abnormalities [48,49,51]. The NAA content in the bilateral hippocampi of the T2DM group was lower than that of the NC group ($p < 0.05$), indicating that hippocampal neurons were damaged or lost in the T2DM rat model, consistent with previous reports [45,52–54]. Additionally, the NAA content in the bilateral hippocampi of the T2DM-ID group was lower than that of the NC group ($p < 0.05$), whereas the NAA level in the bilateral hippocampi did not differ between the T2DM and T2DM-ID groups ($p > 0.05$). Further comparison of NAA/Cr among the three groups revealed that only the NAA/Cr in the left hippocampus of the T2DM-ID group was lower than that in the NC rats ($p < 0.05$), indicating that the degree of loss or damage to hippocampal neurons in the T2DM-ID model was higher than that in the T2DM model. Lateral changes were primarily observed on the left side.

Gut microbes can affect neurodevelopment and brain function through a connecting mechanism that communicates bidirectionally through the GBA [55,56]. The abnormal structure of the gut microbiota may play an important role in T2DM-related brain injury; however, its mechanism of action remains under investigation. Lee et al. [57] confirmed that gut microbiota diversity is positively correlated with brain gray matter volume in patients with depression. Our study showed that the intestinal flora richness index (Chao1 index) was positively correlated with the left hippocampal volume. Therefore, hippocampal atrophy in T2DM and T2DM-ID rat models is related to a decreased diversity of intestinal flora, and the left hippocampus may be more sensitive to this effect. Moreover, the relative abundance of bacteria in the phylum *Firmicutes* was positively correlated with left hippocampal volume in the NC group, whereas the phylum *Proteobacteria* was negatively correlated with left hippocampal volume in the T2DM and T2DM-ID groups. Although the relative abundance of *Actinobacteria* was significantly increased in the T2DM-ID group, we did not determine whether this increase was associated with decreased rat hippocampal volume or NAA levels.

This study revealed that eight genera that were positively correlated with indicators such as rat HV or NAA belonged predominantly (7/8) to the phylum *Firmicutes*; only the *Muribaculaceae* genera belonged to *Bacteroidetes*. The correlation analysis showed that the presence of *Lactobacillus* and *Clostridia_UCG_014* in NC rats was positively correlated with HV and NAA ($r = 0.55$–0.70). *Blautia* was negatively correlated with HV and NAA in the T2DM model. *Escherichia Shigella* was negatively correlated with left HV in the T2DM

model, whereas *Enterococcus* in the T2DM-ID model was negatively correlated with bilateral HVs. *Megamonas* was negatively correlated with right HV in the T2DM-ID model. Luczynski et al. [58] confirmed the atrophy of different hippocampal subregions in germ-free mice. Additionally, the present study showed that intestinal dysbiosis in T2DM rats can lead to hippocampal atrophy and decreased levels of the neuronal marker NAA. Anomalies in the abundance of specific flora such as *Firmicutes*, *Lactobacillus*, and *Blautia* likely play a dominant role. Although dysbiosis of the gut microbiota in diabetes has been confirmed in many studies [4,21,22,45], to the best of our knowledge, few studies have reported an association between dysbiosis of the microbiota in T2DM and hippocampal structure and function. Based on these findings, further research on the mechanisms of gut microbiota and related brain injury in patients with T2DM may have important clinical significance for early disease intervention and drug development.

Despite its comprehensive experimental design, this study had some limitations. For example, the microbiota was detected in the host fecal sample rather than being directly measured from the intestinal mucosa. The microbial equivalence between the two methods requires more scientific evidence for support. In addition, all groups were scanned 7–8 weeks after the STZ injection, before which no MRI examination was performed. Therefore, no dynamic changes in brain structure or function were observed in these models. In addition, we only focused on common bacteria in this study; therefore, more and deeper related research is expected to be conducted in the future. Furthermore, the study did not include tests to analyze cognitive abnormalities, such as the Morris water maze test, or pathological changes in brain tissues, such as hippocampal tissues. Therefore, improvements should be made in future studies. However, our findings provide promising preliminary data demonstrating a potential relationship between the gut microbiota and the volumetric brain and functional correlates within important regions of interest for T2DM, opening new avenues for future investigation into brain aging, gut health, and neural mechanisms of T2DM. This avenue may support the discovery of new targets for microbiome-focused interventions in the treatment and prevention of T2DM.

In conclusion, this study confirmed the compositional abnormality of intestinal bacteria in a T2DM rat model, characterized by an increased relative abundance of bacteria in the phyla *Proteobacteria*, *Actinobacteria*, and *Blautia* and a decreased relative abundance of bacteria in the phyla *Firmicutes*, *Lactobacillus*, and *Clostridia_UCG_014*. Intestinal dysbiosis in T2DM rat models is closely associated with hippocampal atrophy and dysfunction. Considering that the intestinal microecosystem is a large, complex system with self-repairing capabilities, such as the second brain of the human body, deciphering the interaction mechanism between intestinal microorganisms and the central nervous system, starting from the discovery of abnormal intestinal bacteria, will help better understand the etiology of some neuroendocrine diseases, including T2DM, and contribute to the prevention and treatment of diseases. Further relevant research is warranted.

Data availability statement

The data that supports the findings of this study are available in the supplementary material of this article.

Acknowledgment

The authors acknowledge support for this work by grants from the National Natural Science Foundation of China (grant number 82071911) and from the Dalian Science and Technology Innovation Fund (2021JJ12SN38).

CRediT authorship contribution statement

Zhenyang Zhu: Writing – original draft, Validation, Formal analysis. **Qingqing Chen:** Writing – original draft. **Gege Jiang:** Investigation. **Yuan Liang:** Methodology. **Jing Shen:** Writing – review & editing, Formal analysis. **Jianlin Wu:** Writing – review & editing, Supervision, Funding acquisition.

Declaration of competing interest

The authors declare that they have no known competing financial interests or personal relationships that could have appeared to influence the work reported in this paper.

Appendix A. Supplementary data

Supplementary data to this article can be found online at https://doi.org/10.1016/j.heliyon.2024.e33152.

References

[1] M. Zheng, C.D.O. Bernardo, N. Stocks, D. Gonzalez-Chica, Diabetes mellitus diagnosis and screening in Australian general practice: a national study, J. Diabetes Res. 2022 (2022) 1566408.
[2] H. Sun, P. Saeedi, S. Karuranga, M. Pinkepank, IDF diabetes atlas: global, regional and country-level diabetes prevalence estimates for 2021 and projections for 2045, Diabetes Res. Clin. Pract. 183 (2022) 109119.
[3] S. Zhu, Y. Jiang, K. Xu, M. Cui, The progress of gut microbiome research related to brain disorders, J. Neuroinflammation 17 (1) (2020) 1–20.

[4] R.K. West, A. Livny, R. Ravona-Springer, B.B. Bendlin, Higher BMI is associated with smaller regional brain volume in older adults with type 2 diabetes, Diabetologia 63 (11) (2020) 2446–2451.
[5] M. Bogush, N.A. Heldt, Y. Persidsky, Blood brain barrier injury in diabetes: Unrecognized effects on brain and cognition, J. Neuroimmune Pharmacol. 12 (4) (2017) 593–601.
[6] B.L. Furman, Streptozotocin-induced diabetic models in mice and rats, Curr Protoc 1 (4) (2021) e78.
[7] C. Qian, C. Zhu, W. Yu, X. Jiang, High-fat diet/low-dose streptozotocin- induced type 2 diabetes in rats impacts osteogenesis and wnt signaling in bone marrow stromal cells, PLoS One 10 (8) (2015, Aug 21) e0136390.
[8] K. Srinivasan, B. Viswanad, L. Asrat, C.L. Kaul, Combination of high-fat diet-fed and low-dose streptozotocin-treated rat: a model for type 2 diabetes and pharmacological screening, Pharmacol. Res. 52 (4) (2005) 313–320.
[9] R. Chakraborty, V. Lam, S. Kommineni, J. Stromich, Ceftriaxone administration disrupts intestinal homeostasis, mediating noninflammatory proliferation and dissemination of commensal enterococci, Infect. Immun. 86 (12) (2018).
[10] R.Y. Cheng, M. Li, S.S. Li, M. He, Vancomycin and ceftriaxone can damage intestinal microbiota and affect the development of the intestinal tract and immune system to different degrees in neonatal mice, Pathog Dis 75 (8) (2017).
[11] Babiker Saad Almugadam, Peng Yang, Li Tang, Analysis of jejunum microbiota of HFD/STZ diabetic rats, Biomed. Pharmacother. 138 (2021) 111094. Jun.
[12] M. Zhang, X.Y. Lv, J. Li, Z.G. Xu, The characterization of high-fat diet and multiple low-dose streptozotocin induced type 2 diabetes rat model, Exp, Diabetes Res. 2008 (2008) 704045.
[13] X. Luo, Y. Zheng, R. Wen, X. Deng, Effects of ceftriaxone induced intestinal dysbacteriosis on lymphocytes in different tissues in mice, Immunobiology 221 (9) (2016) 994–1000.
[14] M.G.I. Langille, J. Zaneveld, J.G. Caporaso, D. McDonald, Predictive functional profiling of microbial communities using 16S rRNA marker gene sequences, Nat Biotechonol 31 (9) (2013) 814–821.
[15] E. Bolyen, J.R. Rideout, M.R. Dillon, N.A. Bokulich, Reproducible, interactive, scalable and extensible microbiome data science using QIIME 2, Nat. Biotechnol. 37 (8) (2019) 852–857.
[16] B.J. Callahan, P.J. McMurdie, M.J. Rosen, A.W. Han, DADA2: high-resolution sample inference from Illumina amplicon data, Nat. Methods 13 (7) (2016) 581–583.
[17] N.A. Bokulich, B.D. Kaehler, J.R. Rideout, M. Dillon, Optimizing taxonomic classification of marker-gene amplicon sequences with QIIME 2's q2-feature-classifier plugin, Microbiome 6 (1) (2018) 1–17.
[18] Y. Vázquez-Baeza, M. Pirrung, A. Gonzalez, Knight. EMPeror: a tool for visualizing high-throughput microbial community data, GigaScience 2 (1) (2013), 2047-217X-2-16.
[19] E. Kang, Z. Wen, H. Song, K.M. Christian, Adult neurogenesis and psychiatric disorders, Cold Spring Harbor Perspect. Biol. 8 (9) (2016) a019026.
[20] A.C. Tengeler, S.A. Dam, M. Wiesmann, J. Naaijen, Gut microbiota from persons with attention-deficit/hyperactivity disorder affects the brain in mice, Microbiome 8 (1) (2020) 1–14.
[21] F. Liu, J. Li, F. Wu, H. Zheng, Altered composition and function of intestinal microbiota in autism spectrum disorders: a systematic review, Transl. Psychiatry 9 (1) (2019) 1–13.
[22] R. Nagpal, H. Tsuji, T. Takahashi, K. Nomoto, Ontogenesis of the gut microbiota composition in healthy, full-term, vaginally born and breast-fed infants over the first 3 years of life: a quantitative bird's-eye view, Front. Microbiol. 8 (2017) 1388.
[23] S. Westfall, N. Lomis, I. Kahouli, S.Y. Dia, Microbiome, probiotics and neurodegenerative diseases: deciphering the gut brain axis, Cell. Mol. Life Sci. 74 (20) (2017) 3769–3787.
[24] A.L. Cunningham, J.W. Stephens, D.A. Harris, Intestinal microbiota and their metabolic contribution to type 2 diabetes and obesity, J. Diabetes Metab. Disord. 20 (2) (2021) 1855–1870.
[25] S. Yu, Y. Cheng, L. Zhang, Y. Yin, Treatment with adipose tissue-derived mesenchymal stem cells exerts anti-diabetic effects, improves long-term complications, and attenuates inflammation in type 2 diabetic rats, Stem Cell Res. Ther. 10 (1) (2019) 1–18.
[26] M.J. Hossain, M.D. Kendig, M.E. Letton, M.J. Morris, Peripheral neuropathy phenotyping in rat models of type 2 diabetes mellitus: Evaluating uptake of the neurodiab guidelines and identifying future directions, Diabetes Metab. J 46 (2) (2022) 198–221.
[27] R. Tian, X. Liu, L. Jing, et al., Huang-Lian-Jie-Du decoction attenuates cognitive dysfunction of rats with type 2 diabetes by regulating autophagy and NLRP3 inflammasome activation, J. Ethnopharmacol. (2022) 115196.
[28] H.T. Hoang, D.H. Le, T.T.H. Le, T.T.N. Nguyen, Metagenomic 16S rDNA amplicon data of microbial diversity of guts in Vietnamese humans with type 2 diabetes and nondiabetic adults, Data Brief 34 (2021) 106690.
[29] X. He, J. Sun, C. Liu, H. Li, Compositional alterations of gut microbiota in patients with diabetic kidney disease and type 2 diabetes mellitus, Diabetes Metab Syndr Obes 15 (2022) 755.
[30] C. Li, H. Cao, Y. Huan, W. Ji, Berberine combined with stachyose improves glycometabolism and gut microbiota through regulating colonic microRNA and gene expression in diabetic rats, Life Sci. 284 (2021) 119928.
[31] Li Jinyou, Haifeng Lu, Huanwen Wu, L. Chen, Periodontitis in elderly patients with type 2 diabetes mellitus: impact on gut microbiota and systemic inflammation, Aging (Albany NY) 12 (24) (2020) 25956–25980.
[32] R. Rogier, H. Evans-Marin, J. Manasson, P.M. van der Kraan, Alteration of the intestinal microbiome characterizes preclinical inflammatory arthritis in mice and its modulation attenuates established arthritis, Sci. Rep. 7 (1) (2017) 1–12.
[33] J.U. Scher, A. Sczesnak, R.S. Longman, N. Segata, Expansion of intestinal Prevotella copri correlates with enhanced susceptibility to arthritis, Elife 2 (2013) e01202.
[34] J. Geng, Q. Ni, W. Sun, et al., The links between gut microbiota and obesity and obesity related diseases, Biomed. Pharmacother. 147 (2022 Mar) 112678.
[35] Y.S. Park, K. Ahn, K. Yun, et al., Alterations in gastric and gut microbiota following sleeve gastrectomy in high-fat diet-induced obese rats, Sci. Rep. 13 (1) (2023 Dec 2) 21294.
[36] F. Magne, M. Gotteland, L. Gauthier, et al., The Firmicutes/Bacteroidetes ratio: a relevant marker of gut dysbiosis in obese patients? Nutrients 12 (5) (2020) 1474. May 19.
[37] Zhan Zhiyan, Wenxue Liu, Liya Pan, Y. Bao, Overabundance of Veillonella parvula promotes intestinal inflammation by activating macrophages via LPS-TLR4 pathway, Cell Death Dis. 8 (1) (2022) 251.
[38] Hector M. Espiritu, L. Mamuad Lovelia, Seon-Ho Kim, S.J. Jin, Microbiome Shift, diversity, and overabundance of Opportunistic pathogens in Bovine Digital dermatitis revealed by 16S rRNA amplicon sequencing, Animals (Basel) 10 (10) (2020) 1798. Oct 3.
[39] Bruce A.C. Cree, M. Spencer Collin, Varrin-Doyer Michel, S.E. Baranzini, Gut microbiome analysis in neuromyelitis optica reveals overabundance of Clostridium perfringens, Ann. Neurol. 80 (3) (2016) 443–447.
[40] C.M. Hueston, J.F. Cryan, Y.M. Nolan, Stress and adolescent hippocampal neurogenesis: diet and exercise as cognitive modulators, Transl. Psychiatry 7 (4) (2017).
[41] F.N. Jacka, N. Cherbuin, K.J. Anstey, P. Sachdev, Western diet is associated with a smaller hippocampus: a longitudinal investigation, BMC Med. 13 (1) (2015) 1–8.
[42] L. Möhle, D. Mattei, M.M. Heimesaat, S. Bereswill, Ly6Chi monocytes provide a link between antibiotic-induced changes in gut microbiota and adult hippocampal neurogenesis, Cell Rep. 15 (9) (2016) 1945–1956.
[43] S. Gao, Y. Chen, F. Sang, Y. Yang, White matter microstructural change contributes to worse cognitive function in patients with type 2 diabetes, Diabetes 68 (11) (2019) 2085–2094.
[44] J. Zhang, Y. Wang, J. Wang, X. Zhou, White matter integrity disruptions associated with cognitive impairments in type 2 diabetic patients, Diabetes 63 (11) (2014) 3596–3605.

[45] M.L. Callisaya, R. Beare, C. Moran, T. Phan, Type 2 diabetes mellitus, brain atrophy and cognitive decline in older people: a longitudinal study, Diabetologia 62 (3) (2019) 448–458.
[46] Zheng Zhou, Bao Sun, Dongsheng Yu, C. Zhu, Gut microbiota: an important player in type 2 diabetes mellitus, Front. Cell. Infect. Microbiol. 12 (2022) 834485. Feb 15.
[47] Sabari S. Sri, Balasubramani Kiruthika, Iyer Mahalaxmi, H.W. Sureshbabu, Type 2 diabetes (T2DM) and Parkinson's disease (PD): a mechanistic approach, Mol. Neurobiol. 60 (8) (2023) 4547–4573.
[48] Ruiqing Ni, Magnetic resonance imaging in animal models of alzheimer's disease amyloidosis, Int. J. Mol. Sci. 22 (23) (2021) 12768. Nov 25.
[49] Andrew Webb, Alena Shchelokova, Alexey Slobozhanyuk, I. Zivkovic, Novel materials in magnetic resonance imaging: high permittivity ceramics, metamaterials, metasurfaces and artificial dielectrics, Magma 35 (6) (2022) 875–894.
[50] Mullen Michael, Garwood Michael, Contemporary approaches to high-field magnetic resonance imaging with large field inhomogeneity, Prog. Nucl. Magn. Reson. Spectrosc. 120–121 (2020) 95–108. Oct-Dec.
[51] Y. Li, J. Steinberg, Z. Coleman, S. Wang, Proton magnetic resonance spectroscopy detects cerebral metabolic derangement in a mouse model of brain coenzyme a deficiency, J. Transl. Med. 20 (1) (2022) 1–7.
[52] T.M. Shakir, L. Fengli, G. Chenguang, N. Chen, 1H-MR spectroscopy in grading of cerebral glioma: a new view point, MRS image quality assessment, Acta Radiol. Open 11 (2) (2022) 20584601221077068.
[53] Y. He, T. Kosciolek, J. Tang, Y. Zhou, Gut microbiome and magnetic resonance spectroscopy study of subjects at ultra-high risk for psychosis may support the membrane hypothesis, Eur. Psychiatr. 53 (2018) 37–45.
[54] R. Janik, L.A.M. Thomason, A.M. Stanisz, P. Forsythe, Magnetic resonance spectroscopy reveals oral Lactobacillus promotion of increases in brain GABA, N-acetyl aspartate and glutamate, Neuroimage 125 (2016) 988–995.
[55] A.C. Tengeler, S.A. Dam, M. Wiesmann, J. Naaijen, Gut microbiota from persons with attention-deficit/hyperactivity disorder affects the brain in mice, Microbiome 8 (1) (2020) 1–14.
[56] J.R. Kelly, V. O'Keane, J.F. Cryan, G. Clarke, Mood and microbes: gut to brain communication in depression, Gastroenterol. Clin. 48 (3) (2019) 389–405.
[57] S.M. Lee, M.M. Milillo, B. Krause-Sorio, P. Siddarth, Gut microbiome diversity and abundance correlate with gray matter volume (GMV) in older adults with depression, Int. J. Environ. Res. Publ. Health 19 (4) (2022) 2405.
[58] P. Luczynski, S.O. Whelan, C. O'Sullivan, G. Clarke, Adult microbiota-deficient mice have distinct dendritic morphological changes: differential effects in the amygdala and hippocampus, Eur. J. Neurosci. 44 (9) (2016) 2654–2666.